



RESEARCH ARTICLE

Partitioning behavior of short DNA fragments in polymer/salt aqueous two-phase systems

Rafaela Meutelet¹  | Lea J. Bisch¹ | Benedikt C. Buerfent²  | Markus Müller² | Jürgen Hubbuch¹

¹Institute of Process Engineering in Life Sciences, Section IV: Biomolecular Separation Engineering, Karlsruhe Institute of Technology (KIT), Karlsruhe, Germany

²BioEcho Life Sciences GmbH, BioCampus Cologne, Köln, Germany

Correspondence

Jürgen Hubbuch, Institute of Process Engineering in Life Sciences, Section IV: Biomolecular Separation Engineering, Karlsruhe Institute of Technology (KIT), Fritz-Haber-Weg 2, 76131 Karlsruhe, Germany.

Email: juergen.hubbuch@kit.edu

Funding information

BioEcho Life Sciences GmbH

Abstract

The development of liquid biopsy as a minimally invasive technique for tumor profiling has created a need for efficient biomarker extraction systems from body fluids. The analysis of circulating cell-free DNA (cfDNA) is especially promising, but the low amounts and high fragmentation of cfDNA found in plasma pose challenges to its isolation. While the potential of aqueous two-phase systems (ATPS) for the extraction and purification of various biomolecules has already been successfully established, there is limited literature on the applicability of these findings to short cfDNA-like fragments. This study presents the partitioning behavior of a 160 bp DNA fragment in polyethylene glycol (PEG)/salt ATPS at pH 7.4. The effect of PEG molecular weight, tie-line length, neutral salt additives, and phase volume ratio is evaluated to maximize DNA recovery. Selected ATPS containing a synthetic plasma solution spiked with human serum albumin and immunoglobulin G are tested to determine the separation of DNA fragments from the main plasma protein fraction. By adding 1.5% (w/w) NaCl to a 17.7% (w/w) PEG 400/17.3% (w/w) phosphate ATPS, 88% DNA recovery was achieved in the salt-rich bottom phase while over 99% of the protein was removed.

KEYWORDS

aqueous two-phase systems (ATPS), cfDNA extraction, DNA fragment partitioning, high-throughput screening, liquid biopsy

1 | INTRODUCTION

In recent years, liquid biopsy has become a promising diagnostic tool in clinical and precision oncology, as it enables the molecular characterization of tumors without the need for invasive surgical tissue biopsies.^[1] Its minimally invasive nature and easy repeatability offer potential benefits in cancer applications such as early detec-

tion, real-time tumor monitoring, personalized treatment selection, patient response assessment, and detection of minimal residual disease after surgery.^[2] Liquid biopsy is based on analyzing various tumor-derived entities found in body fluids, especially in the bloodstream. One of the most investigated biomarkers is circulating cell-free DNA (cfDNA), more specifically circulating tumor DNA (ctDNA), as its analysis provides not only a comprehensive profile of the tumor genome but also the assessment of intratumor heterogeneity and total tumor burden.^[3,4]

The double-stranded cfDNA is released through apoptosis and necrosis, resulting in high fragmentation with a predominant fragment

Abbreviations: ATPS, aqueous two-phase system; cfDNA, circulating cell-free DNA; ctDNA, circulating tumor DNA; gDNA, genomic DNA; HSA, human serum albumin; IgG, immunoglobulin G; PEG, polyethylene glycol; PCR, polymerase chain reaction; pDNA, plasmid DNA; TLL, tie-line length; V_R , volume ratio.

This is an open access article under the terms of the [Creative Commons Attribution](https://creativecommons.org/licenses/by/4.0/) License, which permits use, distribution and reproduction in any medium, provided the original work is properly cited.

© 2024 The Author(s). Biotechnology Journal published by Wiley-VCH GmbH.

TABLE 1 ATPS-based extraction and purification processes for DNA of different sizes reported in the literature.

DNA size	ATPS	Isolation process	Reference
3×10^7 Da	PEG/Dextran	dsDNA separation from ssDNA	[15]
2×10^7 Da	PEG/Dextran	DNA isolation from microorganisms	[16]
15,000 bp	Triton X-114/PBS	gDNA concentration as biomarker	[17]
–	PEG/phosphate	gDNA removal from protein product	[18]
8500 bp	PEG/phosphate	pDNA purification from lysate	[19]
7796 bp	PEG/phosphate	pDNA partitioning in clean systems/lysate	[20]
6700 bp	PEG/phosphate	pDNA partitioning in clean systems	[21]
–	PEG/phosphate	pDNA partitioning in clean systems/lysate	[22]
6050 bp	EO-PO/Dextran	pDNA purification from lysate	[23]
6050 bp	PEG/sulfate	pDNA purification from lysate	[24]
6050 bp	PEG/citrate/sulfate	pDNA purification from lysate	[25]
3000 bp	PEG/citrate	pDNA purification from lysate	[26]
2686 bp	PEG/PAA/salt	pDNA partitioning in clean systems/lysate	[27]
250–10,000 bp	PEG/PAA/salt	PCR DNA fragment isolation	[28]
145 bp	not described	cfDNA purification from plasma	[29]
20 bp	PEG/sulfate	ss oligonucleotide partitioning	[49]

Abbreviations: bp, base pairs; Da, Dalton; ds, double stranded; EO-PO, ethylene oxide-propylene oxide; gDNA, genomic DNA; pDNA, plasmid DNA; PAA, polyacrylate; PEG, polyethylene glycol; ss, single stranded.

length of 167 bp.^[5] This characteristic length comes from a 147 bp DNA strand wound around a histone octamer, forming a nucleosomal structure attached to a strand of linker DNA. Studies have shown that ctDNA fragments are even shorter than cfDNA, ranging from 132 to 143 bp, which can challenge efficient ctDNA extraction using conventional kits.^[6] Additionally, the dilute ctDNA concentration of around $1\text{--}40\text{ ng mL}^{-1}$ plasma and the high risk of contamination from genomic DNA (gDNA) shed by lysed white blood cells make extraction even more challenging.^[7]

Commercial extraction kits primarily rely on DNA adsorption to solid phases like silica membranes or magnetic beads in the presence of chaotropic salts. If not removed, residual chaotropic salts can inhibit downstream amplification-based analyses. Therefore, standard kits use bind-wash-elute protocols with multiple steps, which can limit cfDNA yields.^[8] Furthermore, a fragment length bias may be introduced due to uneven extraction efficiency of shorter fragments.^[9] These limitations and the lack of standardization hinder the broader implementation of cfDNA analysis in clinical settings, highlighting the need for novel cfDNA extraction methods.^[10,11]

An alternative approach for the integrated extraction and concentration of cfDNA from plasma samples can be achieved using aqueous two-phase systems (ATPS). With their high water content, ATPS offer mild conditions for isolating biomolecules such as cells, viruses, proteins, and nucleic acids.^[12] The extraction using ATPS is rapid, easily scalable, low-cost, and compatible with high-throughput processes.^[13,14] Purification processes using ATPS have already been successfully established for various biomolecules, including nucleic acids like gDNA and plasmid DNA (pDNA). Table 1 lists ATPS-based

extraction and purification processes for DNA of different sizes described in the literature.

Several papers discuss pDNA partitioning in clean systems and pDNA extraction from crude cell lysate for large-scale production in gene therapy.^[19,21,22,31] The literature also covers gDNA isolation and its removal from complex mixtures for target protein purification using ATPS.^[16,18,32] However, little is known about the partitioning behavior of DNA fragments shorter than 200 bp which resemble cfDNA.

As the partitioning behavior in ATPS depends on many factors, including ATPS composition, pH, additives, and target molecule characteristics,^[12] findings for pDNA or gDNA may not apply to shorter cfDNA or ctDNA fragments. Matos et al.^[28] described isolating DNA fragments after polymerase chain reaction (PCR) using ATPS. Fragments up to 6000 bp are recovered in the polyethylene glycol (PEG)-rich top phase of a PEG/polyacrylate system before back-extraction into the salt-rich bottom phase of a PEG/ Na_2SO_4 ATPS. However, the smallest fragments studied are 250 bp, too large to represent cfDNA or the even shorter ctDNA. Additionally, it is uncertain if this method applies to DNA extraction from a complex matrix like plasma. Janku et al.^[29] reported using an ATPS-based kit, PHASIFY MAX, to purify cfDNA from blood for liquid biopsy, promising a 60% yield increase over the silica-based QIAamp Circulating Nucleic Acid kit. The DNA is recovered in the bottom phase, concentrated in the top phase of a second ATPS, and precipitated with isopropanol. The exact ATPS compositions in the kit, commercialized by Phase Scientific (Hong Kong), are undisclosed.

High concentrations of polymer or salt, even if kosmotropic, necessitate a purification step to remove components that could affect downstream analysis. Different purification approaches can be employed

depending on whether the DNA is enriched in the polymer- or salt-rich phase. For example, the PHASIFY MAX kit uses alcohol to precipitate the DNA from the top phase, while desalting resins are suitable for the salt-rich bottom phase.

Because the partitioning of molecules in ATPS is hard to predict and relies heavily on empirical experiments, this paper aims to provide comprehensive insights into the partitioning behavior of short DNA fragments in PEG/salt systems, comparing trends with other reported DNA types. The effects of PEG molecular weight, salt type, tie-line length (TLL), volume ratio (V_R), and neutral salt addition on DNA partitioning and recovery in clean PEG/salt ATPS are investigated. The applicability of the observed partitioning trends to systems containing a synthetic plasma solution is tested, providing a basis for developing an ATPS-based cfDNA extraction process from plasma samples for liquid biopsy.

2 | MATERIAL AND METHODS

2.1 | Chemicals and stock solutions

PEG 200, PEG 400, and PEG 600 of synthesis grade as well as 85% methyl orange dye, human serum albumin (HSA), and immunoglobulin G (IgG) were purchased from Sigma-Aldrich (St. Louis, MO). PEG 1000, $\text{NaH}_2\text{PO}_4 \cdot \text{H}_2\text{O}$, NaCl, KCl, LiCl, MgCl_2 , and CaCl_2 were obtained from Merck KGaA (Darmstadt, Germany). K_2HPO_4 was purchased from VWR International GmbH (Radnor, PA). Stock solutions and buffers were prepared using ultra-pure water as follows: 70% (w/w) PEG, 40% (w/w) phosphate, and 25% (w/w) neutral salt solutions. Phosphate stock solution was prepared by combining 30.91% (w/w) NaH_2PO_4 and 9.09% (w/w) K_2HPO_4 in water to yield pH 7.4. A synthetic plasma electrolyte solution with physiological pH 7.4 was prepared by dissolving 0.9% (w/v) NaCl and 0.2% (w/v) NaHCO_3 in water.

2.2 | DNA fragment preparation

Purified DNA fragments with a length of 160 bp were prepared using pKRha_eGFP_JG 1163 plasmid isolated from *E. coli* as a template DNA. The desired fragment length was amplified by PCR using accordingly designed primer sequences obtained from Merck KGaA. One 50 μL reaction volume contained 50 ng of plasmid, 2 μL of both forward (TAAACGGCCACAAGTTCAG) and reverse (GGGTAGCGCT-GAAGCAC) primer, 10 μL of Hifi Buffer and 0.5 μL of PCR BIO Hifi Polymerase (PCR Biosystems Ltd., London, UK) as well as DNase-free water. Twenty-four cycles consisting of heat denaturation at 95°C for 3 s, primer annealing at 60°C for 30 s, and elongation at 72°C for 10 s were carried out on a C1000 Touch Thermal Cycler (Bio-Rad Laboratories GmbH, Hercules, CA). The PCR product was purified using the Wizard SV Gel and PCR Clean-Up System (Promega GmbH, Madison, WI) and diluted with DNase-free water to create a 10 ng μL^{-1} DNA fragment stock solution.

2.3 | Liquid handling station

A Tecan Freedom EVO system (Tecan, Crailsheim, Germany) was used as a liquid handling platform for automated ATPS experiments. The system set-up and liquid handling calibration procedure were described in earlier work.^[33] The robotic workstation was controlled using Evoware 2.4 SP3. Importing pipetting volumes and exporting photometric data were done using Excel 2007 (Microsoft Corporation, Redmond, WA).

2.4 | ATPS screening procedure

Automated routines adapted from previous methods developed by our group were used for binodal curve and tie-line determination^[34,33] as well as for DNA partitioning experiments in different ATPS.^[18] Binodal points were identified using the cloud point method and fitted to the following equation given by Merchuk, Andrews, and Asenjo:^[35]

$$x_{\text{PEG}} = a * \exp\left(x_{\text{salt}}^{0.5} + c * x_{\text{salt}}^3\right) \quad (1)$$

Tie-lines were determined as described by Diederich et al.,^[13] except that methyl orange dye was used instead of methyl violet for mass balance measurements and subsequent V_R calculations. System points with V_R near 1 were selected to investigate the DNA fragment partitioning behavior in clean ATPS. Various parameters including the molecular weight of PEG, TLL, and the type and concentration of neutral salt additives, were varied to evaluate the effects on DNA partitioning and recovery in the ATPS top and bottom phases. A total of 600 μL ATPS with a final concentration of 100 ng mL^{-1} 160 bp DNA were prepared in 1 mL 96-deep well polypropylene plates (Thermo Fisher Scientific Inc., Waltham, MA) by adding stock solutions in the following order: water, phosphate salt, additive salt, and PEG. This spike-in concentration was chosen to mimic the realistic concentration range of cfDNA in blood samples. ATPS were mixed for 1 min at 1100 rpm on an orbital shaker before spiking with DNA stock solution, mixing for incubation, and centrifuging at 4000 rpm for 5 min to achieve phase separation. One hundred microliters were sampled from top and bottom phases using an optimized sampling method^[33] and desalted using proprietary purification plates (BioEcho Life Sciences GmbH, Cologne, Germany) to reduce interference by the phase-forming components for subsequent DNA quantification. Phase volumes and the DNA concentration in each phase were measured in triplicate. DNA partitioning trends were assessed using DNA recovery as a percentage instead of concentration, as the latter depends on phase volume, which varies across experiments. DNA recoveries in the top and bottom phases were calculated by multiplying the measured DNA concentrations with the respective phase volumes and dividing by the amount of input DNA. Similar partitioning experiments were performed by spiking selected ATPS with a final concentration of 2.5 mg mL^{-1} of either HSA or IgG instead of DNA to investigate the partitioning behavior of the main plasma protein fractions.

2.5 | Separation experiments with synthetic plasma

Separation experiments with synthetic plasma were conducted manually in 1.5 mL reaction tubes for selected ATPS. Six hundred microliters ATPS with a final concentration of 100 ng mL⁻¹ 160 bp DNA were prepared by adding stock solutions in the following order: plasma electrolyte solution, phosphate salt, additive salt, and PEG. After brief vortexing of the phase-forming components, a protein mix consisting of 60 mg mL⁻¹ HSA and 15 mg mL⁻¹ IgG was added to achieve a final protein concentration of 10 mg mL⁻¹ in the ATPS. Lastly, ATPS were spiked with 160 bp DNA fragments, vortexed for incubation, and centrifuged in a microcentrifuge at 4000 rpm for 5 min for phase separation. Phase volumes were determined visually. Phase samples were not desalted but diluted tenfold in water to reduce interference of the phase-forming components with DNA and protein quantification analyses. Adequate blank phases were used for background correction and the same blank phases were spiked with a defined amount of DNA as references for recovery calculations.

2.6 | Analytical methods

2.6.1 | DNA quantification

The DNA concentration in the ATPS top and bottom phases was measured using the Quant-iT PicoGreen dsDNA HS assay kit (Thermo Fisher Scientific Inc.). Black 96-well half-area polystyrene microplates (Greiner Bio-One, Kremsmünster, Austria) (50 μ L per well) and black 384-well microplates (10 μ L per well) were used for the automated screening and the manually prepared ATPS, respectively. Samples were analyzed against blanks with similar phase composition but without DNA to account for interference. Four-point calibration curves were constructed by spiking 160 bp DNA fragments into reference top and bottom phases. For the automated screening, the PEG and salt concentrations in these reference phases were set to half the average concentrations in the top and bottom phases of the screened system points. This was done to ensure the reference phases remained in the one-phase region and to prevent DNA precipitation upon spiking. ATPS samples were diluted 1:2 with water after desalting to match the reference phase composition. Fluorescence measurements were performed according to the manufacturer's instructions after a 2-minute incubation.

2.7 | Agarose gel electrophoresis

The DNA fragment partitioning into the top and bottom phases was visualized on 2% agarose gels stained with 1 μ L mL⁻¹ Midori Green (Nippon Genetics Europe, Dürren, Germany). Electrophoresis was carried out at 120 V for 40 min using TAE as a running buffer. The gels were visualized and photographed using the GelDoc Go Gel Imaging System by Bio-Rad (Hercules, CA).

2.7.1 | Protein quantification

Protein concentrations in the ATPS top and bottom phases from the automated screening were determined by UV-VIS absorbance at 280 nm in Greiner Bio-One 350 μ L-polystyrene UV Star plates (300 μ L per well). The samples from the manually prepared separation experiments were measured using the NanoDrop 2000/2000c. ATPS samples were diluted tenfold in water rather than desalted to reduce polymer and salt interference while avoiding protein loss.

3 | RESULTS AND DISCUSSION

3.1 | ATPS characterization

Phase diagrams were determined for several PEG/salt combinations using automatic routines on the liquid handling station to select appropriate system points for partitioning experiments (Figure S1). The binodal curves match those of Effio et al.,^[18] confirming the robustness of the automated method developed by Oelmeier, Dismer, and Hubbuch.^[33] As PEG molecular weight increases, the curves shift toward the origin, indicating that fewer phase-forming components are needed for phase separation. Larger PEG chains have a more hydrophobic character and lower solubility in water, correlating with a higher excluded volume and increased salting-out ability. This leads to greater incompatibility between the polymer and salt components, resulting in a larger two-phase region and steeper tie-line slopes.^[36,37] Adding NaCl also causes a slight shift of the binodal curves toward the origin. This shift is consistent with the literature and can be explained by the increased salting-out effect upon NaCl addition.^[36]

3.2 | Effect of PEG molecular weight on DNA fragment partitioning

The partitioning behavior of a pure 160 bp DNA fragment in clean ATPS was investigated by varying PEG molecular weight and TLL. Systems points with V_R near 1 were chosen following the characterization experiments and spiked with 100 ng mL⁻¹ DNA. Figure 1 shows the DNA distribution in PEG 200, PEG 400, PEG 600, and PEG 1000/phosphate systems at pH 7.4. The colored dots along the binodal curve represent the DNA recovery in the top and bottom phases of the system points marked with a cross on the corresponding tie-line. The axes show the concentrations of the phase-forming components plotted against each other in weight percent. For exact recovery values, ATPS compositions, and TLL, see Table S1.

A trend of top-phase DNA fragment partitioning was observed for PEG 200 and PEG 400 ATPS, while bottom-phase partitioning was favored for PEG 600 and PEG 1000 ATPS. As PEG molecular weight increases, the exclusion volume decreases, reducing space in the top phase for DNA fragments.^[25] This effect seems consistent across different DNA sizes, with studies reporting that a PEG

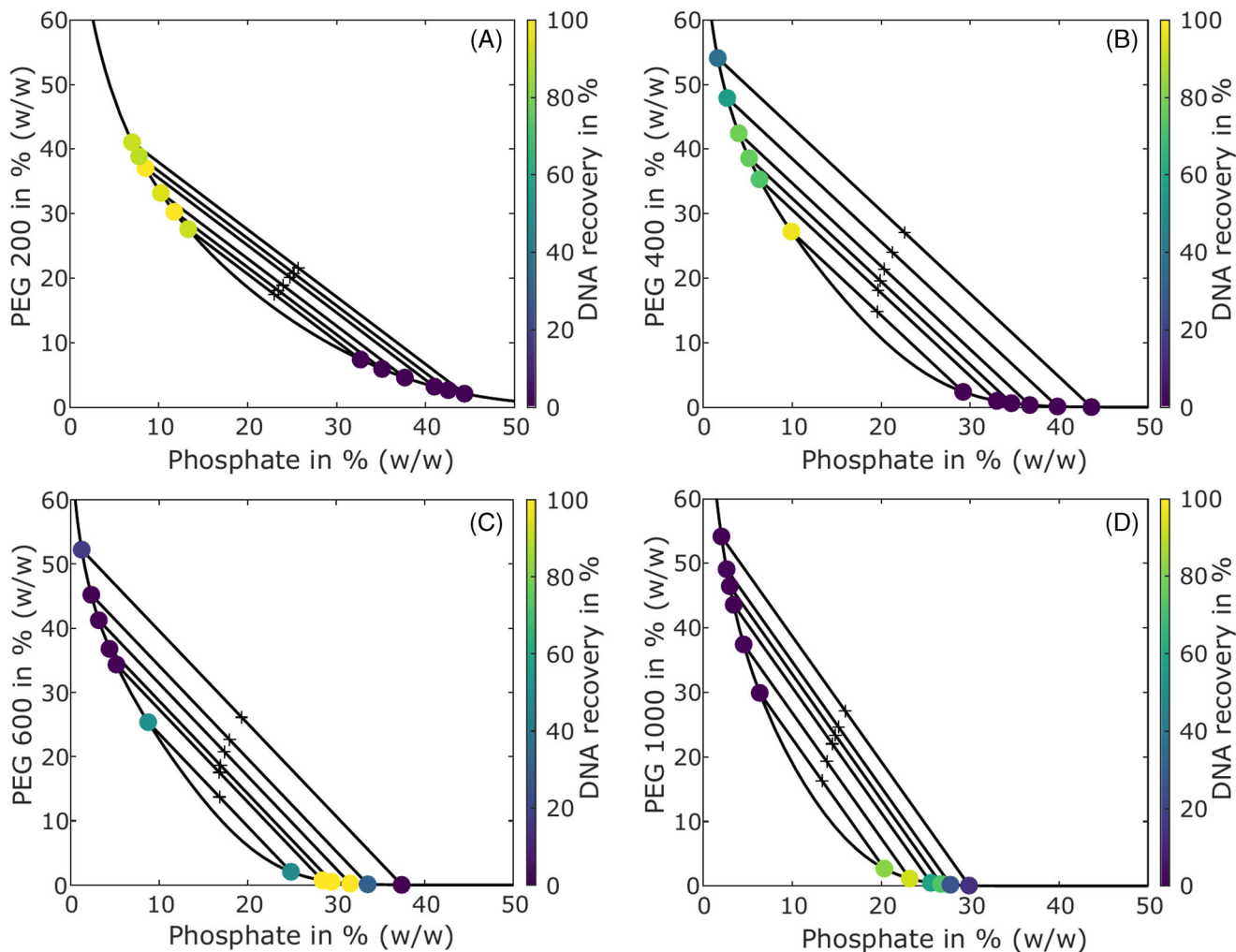


FIGURE 1 Partitioning of a 160 bp DNA fragment in selected PEG/phosphate ATPS at pH 7.4. Binodal curves and tie-lines are shown, with “x” marking the system compositions of the screened ATPS spiked with 100 ng mL^{-1} DNA. Color-coded dots along the binodal curve illustrate the DNA recovery in the respective top and bottom phases. Each partitioning experiment was carried out in triplicate.

molecular weight of 600 g mol^{-1} reliably excludes pDNA ranging from 2700 to 8500 bp from the top phase of PEG/phosphate ATPS.^[19,24] Additionally, higher molecular weight polymers increase the hydrophobicity of the top phase, making it less suitable for hydrophilic DNA fragments.^[30]

The partitioning behavior of nucleic acids is determined not only by hydrophobic forces but also by electrostatic ones. The strong one-sided partitioning observed is partly due to the high net charge of DNA, causing electrostatic repulsion from the ion-rich bottom phase.^[38] Except for one PEG 600 system point near the binodal, where DNA was partitioned evenly, all systems showed one-sided distribution. This indicates that the interplay between hydrophobic and electrostatic forces governs the partitioning behavior of short DNA fragments, as it does for longer DNA forms.^[39] When there is enough “space” in the top phase to accommodate the DNA, it will partition away from the salt-rich bottom phase. Beyond a certain exclusion limit, here at PEG 600, DNA distributes into the bottom phase, despite the electrostatic repulsion with the phosphate anions. When top and bottom phase composi-

tions are too similar, the partitioning effects balance each other out, resulting in a more even DNA distribution.

3.3 | Effect of TLL on DNA fragment recovery

DNA fragment recovery reached 90%–100% in the top phase of the tested PEG 200 ATPS (Figure 1A). A trend of decreasing total recovery with increasing TLL was observed for the tested PEG molecular weights. The longer the tie-line, the higher the phosphate concentration in the bottom phase and PEG concentration in the top phase, implying an intrinsic reduction of water content.^[40] High salt concentrations lead to a strong salting-out effect which lowers the solubility of additional solutes in the bottom phase, potentially causing precipitation even at DNA input concentrations as low as 100 ng mL^{-1} . PEG is known to precipitate nucleic acids,^[41] an effect that increases with PEG molecular weight.^[42] This explains the decreased DNA recovery with increasing TLL and why this trend was not observed for PEG 200,

since its exclusion limit allows the partitioning of the 160 bp fragment into the top phase without precipitation. Despite no visible interphase, it is presumed that the DNA missing from the mass balance accumulated at the interface between the top and bottom phases when both the exclusion effect of the polymer phase and the salting-out effect of the salt phase were too high.

A system point on a shorter tie-line should be selected to avoid precipitation due to the phase-forming components. However, points too close to the binodal curve, with similar top and bottom phase compositions, may lead to even target distribution, longer phase separation times, and reduced process robustness. This should be considered when working with biological samples like plasma that can vary in composition. Similar findings for pDNA in PEG/polyacrylate/salt ATPS were reported by Johansson et al.^[27] Thus, an optimal TLL must be identified for one-sided DNA recovery while minimizing DNA loss due to precipitation. This is especially important for cfDNA extraction for early cancer detection, as cfDNA levels in plasma are typically minimal, and losing DNA during the preanalytical steps could compromise detection.^[10]

3.4 | Effect of neutral salt additives on DNA phase transition

Both gDNA and pDNA undergo a drastic phase transition from top to bottom phase upon adding neutral salt to PEG/salt ATPS for PEG with a molecular weight of less than 600 g mol⁻¹. This is likely due to uneven ion partitioning in ATPS, altering the physicochemical properties of the phases.^[18,42] The applicability of this directed partitioning behavior to cfDNA-like fragments was investigated using different neutral salts. Figure 2A–C shows the recovery of 100 ng mL⁻¹ spiked 160 bp DNA fragment in the top and bottom phases of a 17.7% (w/w) PEG 400/17.3% (w/w) phosphate ATPS with the addition of various neutral salts up to 1.5% (w/w). This system composition was selected based on the high top phase recovery of 98% achieved in previous partitioning experiments without neutral salts. The slight shift of the binodal curve due to the salting-out ability of the added salts was not considered here due to the low salt amounts added, but changes in phase volume ratios were taken into account.^[36,42]

A clear phase transition from top to bottom was observed with 1.5% (w/w) KCl, but total DNA recovery was only 58%, suggesting DNA may have accumulated at the interface between the top and bottom phases rather than fully partitioning into the bottom phase. The lack of a visible interphase made sampling and DNA quantification infeasible, though other studies confirm interphase accumulation at higher pDNA concentrations.^[22] The phase transition was more pronounced for systems containing NaCl or LiCl, occurring at 1% (w/w) added salt. For 1.5% (w/w) NaCl and LiCl, bottom phase recoveries were 83% and 73% respectively, while top phase recoveries fell below the detection limit. This may be attributed to the chloride anions' preferential partitioning into the PEG-rich top phase, leading to DNA exclusion from the top phase into the interphase. As more neutral salt is added, the exclusion effect of the chloride anions becomes stronger and more cations facilitate the transition of the DNA from the interphase into the

bottom phase.^[43] However, adding even more salt may not necessarily increase bottom-phase recovery due to solubility limitations and DNA precipitation.

Systems containing MgCl₂ or CaCl₂ did not exhibit a phase transition at tested concentrations. Instead, total DNA recovery decreased, with only 56% and 25% recovered at 1.5% (w/w) MgCl₂ or CaCl₂, respectively. Precipitation was visible even in blanks without DNA containing MgCl₂ or CaCl₂, and to a lesser extent LiCl, suggesting the solubility limit was exceeded. The precipitating salts may lead to DNA co-precipitation, explaining the low recoveries. The observed precipitation correlates with the position of the chloride counter-cations in the Hofmeister series. The Mg²⁺ and Ca²⁺ cations are more chaotropic than the other tested cations, exhibiting higher incompatibility with the PEG and phosphate phases.

The NaCl-induced phase transition was visualized using agarose gel electrophoresis to qualitatively confirm the fluorescent dye measurements (Figure S2). No band was visible in the bottom phase samples with 0% and 0.5% (w/w) added salt, whereas a band appeared only in the bottom phase for samples with over 1% (w/w) NaCl. The low resolution is attributed to the low DNA concentration in the ATPS.

These results demonstrate that short DNA fragments behave similarly to other negatively charged molecules when neutral salt is added to PEG/salt ATPS. Among the salts tested, NaCl was the most effective in directing DNA partitioning from the top to the bottom phase. NaCl did not cause visible precipitation and a bottom phase recovery of 83% was achieved with just 1.5% (w/w) added salt, corresponding to 0.3 M.

3.5 | Effect of phase volume ratio on DNA concentration

In addition to capturing target molecules from complex mixtures, ATPS offer the advantage of integrating a volume reduction step by adjusting the phase volume ratio. Theoretically, all system points along the same tie-line result in the same target distribution regardless of the volume ratio, as the top and bottom phases share the same equilibrium composition.^[44] This means a target molecule can be concentrated by reducing the volume of the phase where it accumulates. Three ATPS along the same tie-line with PEG 400/phosphate compositions of 12.2% (w/w)/21.0% (w/w), 17.7% (w/w)/17.3% (w/w), and 24.0% (w/w)/13.0% (w/w) and respective top to bottom phase V_R of 0.5, 1, and 2.5 were spiked with 100 ng mL⁻¹ DNA and up to 1.5% (w/w) NaCl. Figure 2D–F shows the recovery in the top and bottom phases and the total DNA recovery for these system points.

Contrary to expectations, the partitioning behavior of pure DNA fragments in clean ATPS was not independent of V_R . Previous results showed a phase transition upon NaCl addition for $V_R = 1$, with DNA recovery shifting from 94% in the top phase to 82% in the bottom phase after adding 1.5% (w/w) NaCl. However, partitioning and total recovery differed for the other two V_R values tested. Luechau et al.^[20] also observed varying partition behavior of pDNA in PEG 300/phosphate ATPS with different V_R , attributing it to changes in the PEG/salt ATPS

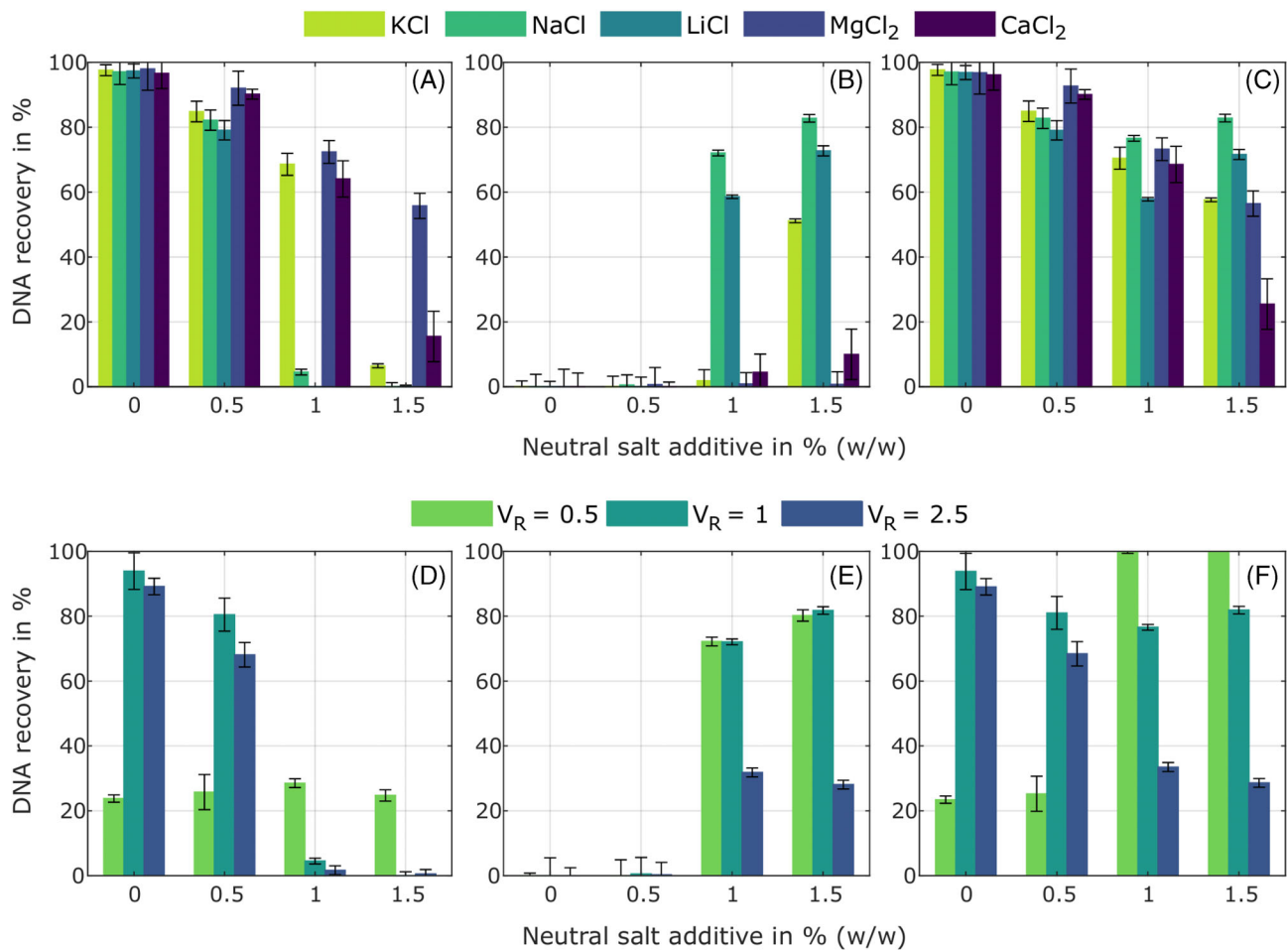


FIGURE 2 Partitioning of 160 bp DNA fragment in a 17.7% (w/w) PEG 400/17.3% (w/w) phosphate ATPS with varying neutral salt additives: (A) top phase, (B) bottom phase, and (C) total recovery. Partitioning of 160 bp DNA fragment in ATPS along the same tie-line with varying phase volume ratio (V_R) for different NaCl concentrations: (D) top phase, (E) bottom phase, and (F) total recovery. The respective PEG 400/phosphate compositions for $V_R = 0.5, 1,$ and 2.5 are 12.2% (w/w)/21.0% (w/w), 17.7% (w/w)/17.3% (w/w), and 24.0% (w/w)/13.0% (w/w). Systems were spiked with 100 ng mL^{-1} DNA in duplicate.

properties induced by the solute. This explanation is unlikely to apply here, as the systems investigated contain only PEG 400 and salt, with a negligible amount of pure spiked DNA.

Instead of a DNA concentration in the top phase of the $V_R = 0.5$ system point without NaCl, recovery dropped to 24%. Systems with added salt exhibited a nearly constant top phase recovery, rather than the drastic phase switch observed for $V_R = 1$ and 2.5 . This suggests that reducing the volume of the phase where DNA is expected to accumulate might lead to DNA loss rather than concentration. It appears that the solubility limit is reached as the phase volume decreases, making the partitioning coefficient dependent on DNA concentration. However, it remains unclear whether DNA exceeding the solubility limit precipitates or accumulates at the interphase, where it is difficult to sample and hence not detectable. The observation that DNA recovery in the bottom phase of the $V_R = 0.5$ system with over 1% (w/w) added salt reaches up to 80%, while top phase recovery remains constant at around 24%, suggests DNA may have migrated from the interphase to the bottom phase. Again, this is likely due to the preferential ion distribution upon NaCl addition, making bottom phase distribution more favorable for DNA fragments.

DNA was undetectable in the bottom phase of all system points containing less than 1% (w/w) added NaCl, regardless of the V_R . At 1.5% (w/w) NaCl, bottom phase recovery was about 80% for the $V_R = 1$ and 0.5 ATPS, but only 28% for $V_R = 2.5$, despite expectations of DNA concentration in the bottom phase. This discrepancy may result from the higher PEG input concentration required for ATPS with a higher V_R . High polymer concentrations with adequate salt concentrations can favor DNA condensation, leading to precipitation.^[45] Since the top and bottom phases of system points along one tie-line should have the same compositions, DNA may precipitate before phase separation.

3.6 | Selective DNA phase transition by NaCl addition

Further partitioning experiments with plasma proteins assessed the selectivity of the NaCl-induced DNA phase switch. To avoid potential interactions between the components, DNA, HSA, and IgG were spiked separately into 17.7% (w/w) PEG 400/17.3% (w/w) phosphate ATPS containing NaCl concentrations up to 1.5% (w/w). The recoveries in the

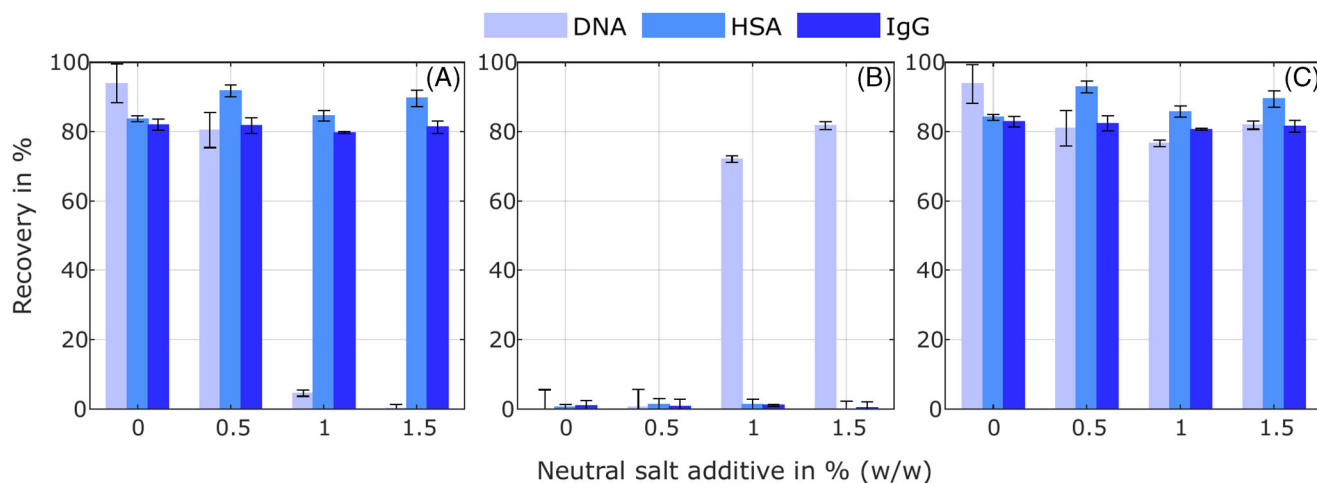


FIGURE 3 Partitioning of 160 bp DNA fragment, HSA, and IgG in a 17.7% (w/w) PEG 400/17.3% (w/w) phosphate ATPS with varying NaCl concentrations: (A) top phase, (B) bottom phase, and (C) total recovery. Systems were made in triplicate and spiked with either 100 ng mL⁻¹ DNA, 2.5 mg mL⁻¹ HSA, or 2.5 mg mL⁻¹ IgG.

top and bottom phases and total recoveries are shown in Figure 3. The x-axis indicates the NaCl concentrations in weight percent.

Protein concentrations remained below the detection limit in the bottom phases of the investigated systems, whereas 82% of spiked DNA was recovered in the bottom phase with 1.5% (w/w) NaCl. HSA recovery in the top phase ranged between 84% and 92%, while IgG top phase recovery was around 81% across the investigated NaCl range. This suggests hydrophobic interactions play a larger role in protein distribution than electrostatic effects, at least at the investigated salt concentrations.^[46] In previous studies, where gDNA was seen as a contaminant to protein targets, adding NaCl to the ATPS helped improve purification efficiency.^[18] Here, a DNA-selective phase transition could be utilized to purify cfDNA from protein contaminants in a plasma sample by enriching the DNA in the protein-depleted bottom phase while retaining an acceptable yield.

3.7 | DNA fragment separation from synthetic plasma

Promising system points from pure component experiments were tested with a synthetic plasma matrix to evaluate whether potential interactions between plasma proteins and DNA could alter the observed partitioning behaviors. The matrix, composed of a plasma-like electrolyte solution, was used to substitute water in the selected ATPS. The systems were spiked with the two main plasma protein fractions HSA and IgG, and with DNA, only after premixing the phase-forming components to rule out the possibility of initial precipitation due to the high PEG and salt concentrations used. The top and bottom phase recoveries are listed in Table 2 along with the exact ATPS compositions. Values below the detection limit are reported as zero.

The DNA and protein partitioning behavior in PEG 400 systems with synthetic plasma matched those of clean systems with separate components. DNA partitioning remained unchanged, indicating that interactions with proteins or electrolytes did not play a significant

role at the tested concentrations. Adding 1.5% (w/w) NaCl drastically changed DNA distribution without affecting protein distribution, confirming the selectivity of the NaCl-induced phase switch for systems with mixed components. This enabled a DNA recovery of up to 88% in the virtually protein-free bottom phase of the PEG 400/phosphate system. Another way to separate the DNA fragments from the protein fraction is to use the precipitating ability of higher molecular weight PEG to an advantage. Because of the reduction of excluded volume and increasing upper phase hydrophobicity^[47] as well as the solubility limitation in the bottom phase, 42.2% of the total protein precipitated and formed a visible interphase in the tested PEG 1000 system. Only 9.6% of the protein partitioned into the bottom phase, where 87% of the DNA was recovered.

These partitioning experiments with synthetic plasma offer promising tools for cfDNA separation from plasma samples, such as selectively switching DNA distribution or increasing protein precipitation. However, more research is needed to confirm their applicability to complex plasma samples, where protein concentration is 6–8 times higher than the protein input tested here.^[48] Also, cfDNA concentrations in plasma vary widely based on cancer type and stage, exceeding 100 ng mL⁻¹ only in some types of advanced cancer cases. Additionally, the nucleosomal nature of cfDNA might affect partitioning, as histone-bound DNA could behave differently if no lysis step is performed. However, a lysis step could alter protein distribution and introduce new components to the ATPS that must be accounted for.

4 | CONCLUSIONS

This work presents the basics of short DNA fragment partitioning in PEG/phosphate ATPS, laying the groundwork for developing an ATPS-based cfDNA extraction system from plasma for liquid biopsy. Distribution experiments with pure components were carried out on a high-throughput screening platform to assess the effect of PEG molecular weight, TLL, neutral salt additive, and phase volume ratio on DNA

TABLE 2 160 bp DNA fragment and total protein recoveries in the top and bottom phases of selected PEG/phosphate ATPS made with a synthetic plasma matrix.

ATPS composition in % (w/w)			Top phase recovery in %		Bottom phase recovery in %	
PEG	Phosphate	NaCl	160 bp DNA	Protein ^a	160 bp DNA	Protein ^a
17.7 ^b	17.3	0	96.2 ± 10.3	72.0 ± 0.5	0	1.0 ± 0.1
17.7 ^b	17.3	1.5	0	73.7 ± 0.4	87.7 ± 8.8	1.0 ± 0.1
19.5 ^c	13.8	0	0	32.6 ± 0.3	86.6 ± 4.0	9.6 ± 0.3

^aHSA:IgG spike-in ratio of 4:1 for a final protein concentration of 10 mg mL⁻¹.

^bPEG 400.

^cPEG 1000.

partitioning and recovery. The partitioning behavior aligns with previous pDNA studies. Short DNA fragments distribute into the bottom phase for higher molecular weight PEG and into the top phase for PEG smaller than 600 g mol⁻¹. Minimizing DNA loss from precipitation can be managed by selecting system points on shorter tie-lines and considering solubility limits when varying the phase volume ratio. Adding neutral salts like NaCl can selectively direct DNA fragments into the protein-depleted bottom phase. Separation experiments with a synthetic plasma matrix containing HSA and IgG resulted in 88% DNA recovery and nearly 100% protein removal in the salt-rich bottom phase, demonstrating the potential of ATPS for cfDNA extraction from plasma.

AUTHOR CONTRIBUTIONS

Rafaela Meutelet: Conceptualization (equal); formal analysis (lead); investigation (equal); methodology (lead); project administration (equal); visualization (lead); writing—original draft (lead); writing—review and editing (lead). Lea J. Bisch: Formal analysis (supporting); investigation (equal); methodology (Supporting); writing—review and editing (supporting). Benedikt C. Buerfent: Project administration (supporting); resources (lead); supervision (supporting); writing—review and editing (supporting). Markus Müller: Project administration (supporting); resources (supporting); supervision (supporting); writing—review and editing (supporting). Juergen Hubbuch: Conceptualization (equal); project administration (equal); supervision (lead); writing—review and editing (supporting).

ACKNOWLEDGMENTS

The authors gratefully acknowledge BioEcho Life Sciences GmbH (Köln, Germany) for their sponsorship, material supply, and insightful support. Thanks also to Nicola Böhner for her assistance in designing and producing the DNA fragment. The authors declare no conflict of interest.

CONFLICT OF INTEREST STATEMENT

The authors declare no conflicts of interest.

DATA AVAILABILITY STATEMENT

The data that support the findings of this study are available from the corresponding author upon reasonable request.

ORCID

Rafaela Meutelet  <https://orcid.org/0000-0002-7961-2477>

Benedikt C. Buerfent  <https://orcid.org/0000-0002-3739-6112>

REFERENCES

- Heitzer, E., Haque, I. S., Roberts, C. E. S., & Speicher, M. R. (2019). Current and future perspectives of liquid biopsies in genomics-driven oncology. *Nature Reviews Genetics*, 20(2), 71–88. <https://doi.org/10.1038/s41576-018-0071-5>
- Alix-Panabières, C., & Pantel, K. (2021). Liquid biopsy: From discovery to clinical application. *Cancer Discovery*, 11(4), 858–873. <https://doi.org/10.1158/2159-8290.CD-20-1311>
- Bettegowda, C., Sausen, M., Leary, R. J., Kinde, I., Wang, Y., Agrawal, N., Bartlett, B. R., Wang, H., Luber, B., Alani, R. M., Antonarakis, E. S., Azad, N. S., Bardelli, A., Brem, H., Cameron, J. L., Lee, C. C., Fecher, L. A., Gallia, G. L., Gibbs, P., & Diaz, L. A. (2014). Detection of circulating tumor DNA in early- and late-stage human malignancies. *Science Translational Medicine*, 6(224), 224ra24. <https://doi.org/10.1126/scitranslmed.3007094>
- De Mattos-Arruda, L., Weigelt, B., Cortes, J., Won, H. H., Ng, C. K. Y., Nuciforo, P., Bidard, F.-C., Aura, C., Saura, C., Peg, V., Piscuoglio, S., Oliveira, M., Smolders, Y., Patel, P., Norton, L., Taberner, J., Berger, M. F., Seoane, J., & Reis-Filho, J. S. (2014). Capturing intra-tumor genetic heterogeneity by de novo mutation profiling of circulating cell-free tumor DNA: A proof-of-principle. *Annals of Oncology*, 25(9), 1729–1735. <https://doi.org/10.1093/annonc/mdu239>
- Lo, Y. M. D., Chan, K. C. A., Sun, H., Chen, E. Z., Jiang, P., Lun, F. M. F., Zheng, Y. W., Leung, T. Y., Lau, T. K., Cantor, C. R., & Chiu, R. W. K. (2010). Maternal plasma DNA sequencing reveals the genome-wide genetic and mutational profile of the fetus. *Science Translational Medicine*, 2(61), 61rap1. <https://doi.org/10.1126/scitranslmed.3001720>
- Underhill, H. R., Kitzman, J. O., Hellwig, S., Welker, N. C., Daza, R. M., Baker, D. N., Gligorich, K. M., Rostomily, R. C., Bronner, M. P., & Shendure, J. (2016). Fragment length of circulating tumor DNA. *PLOS Genetics*, 12(7), e1006162. <https://doi.org/10.1371/journal.pgen.1006162>
- Volckmar, A.-L., Sültmann, H., Riediger, A., Fioretos, T., Schirmacher, P., Endris, V., Stenzinger, A., & Dietz, S. (2018). A field guide for cancer diagnostics using cell-free DNA: From principles to practice and clinical applications. *Genes Chromosomes and Cancer*, 57(3), 123–139. <https://doi.org/10.1002/GCC.22517>
- Diefenbach, R. J., Lee, J. H., Kefford, R. F., & Rizos, H. (2018). Evaluation of commercial kits for purification of circulating free DNA. *Cancer Genetics*, 228–229, 21–27. <https://doi.org/10.1016/j.cancergen.2018.08.005>
- Devonshire, A. S., Whale, A. S., Gutteridge, A., Jones, G., Cowen, S., Foy, C. A., & Huggett, J. F. (2014). Towards standardisation of cell-free DNA measurement in plasma: Controls for extraction efficiency, fragment

- size bias and quantification. *Analytical and Bioanalytical Chemistry*, 406(26), 6499–6512. <https://doi.org/10.1007/s00216-014-7835-3>
10. Grözl, D., Hauch, S., Schlumpberger, M., Guenther, K., Voss, T., Sprenger-Haussels, M., & Oelmüller, U. (2018). Liquid biopsy preservation solutions for standardized pre-analytical workflows – Venous whole blood and plasma. *Current Pathobiology Reports*, 6(4), 275–286. <https://doi.org/10.1007/S40139-018-0180-Z/TABLES/2>
 11. Sorber, L., Zwaenepoel, K., Deschoolmeester, V., Roeyen, G., Lardon, F., Rolfo, C., & Pauwels, P. (2017). A comparison of cell-free DNA isolation kits. *Journal of Molecular Diagnostics*, 19(1), 162–168. <https://doi.org/10.1016/j.jmoldx.2016.09.009>
 12. Hatti-Kaul, R. (2001). Aqueous two-phase systems—A general overview. *Molecular Biotechnology*, 19(3), 269–278. <https://doi.org/10.1385/MB:19:3:269>
 13. Diederich, P., Amrhein, S., Hämmerling, F., & Hubbuch, J. (2013). Evaluation of PEG/phosphate aqueous two-phase systems for the purification of the chicken egg white protein avidin by using high-throughput techniques. *Chemical Engineering Science*, 104, 945–956. <https://doi.org/10.1016/j.ces.2013.10.008>
 14. Rosa, P. A. J., Ferreira, I. F., Azevedo, A. M., & Aires-Barros, M. R. (2010). Aqueous two-phase systems: A viable platform in the manufacturing of biopharmaceuticals. *Journal of Chromatography A*, 1217(16), 2296–2305. <https://doi.org/10.1016/J.CHROMA.2009.11.034>
 15. Alberts, B. M. (1967). Efficient separation of single-stranded and double-stranded deoxyribonucleic acid in a dextran-polyethylene glycol two-phase system*. *Biochemistry*, 6(8), 2527–2532.
 16. Rudin, L., & Albertsson, P. Å. (1967). A new method for the isolation of deoxyribonucleic acid from microorganisms. *Biochimica et Biophysica Acta (BBA)—Nucleic Acids and Protein Synthesis*, 134(1), 37–44. [https://doi.org/10.1016/0005-2787\(67\)90087-1](https://doi.org/10.1016/0005-2787(67)90087-1)
 17. Mashayekhi, F., Meyer, A. S., Shiigi, S. A., Nguyen, V., & Kamei, D. T. (2009). Concentration of mammalian genomic DNA using two-phase aqueous micellar systems. *Biotechnology and Bioengineering*, 102(6), 1613–1623. <https://doi.org/10.1002/BIT.22188>
 18. Ladd Effio, C., Wenger, L., Ötes, O., Oelmeier, S. A., Kneusel, R., & Hubbuch, J. (2015). Downstream processing of virus-like particles: Single-stage and multi-stage aqueous two-phase extraction. *Journal of Chromatography A*, 1383, 35–46. <https://doi.org/10.1016/J.CHROMA.2015.01.007>
 19. Ribeiro, S. C., Monteiro, G. A., Cabral, J. M. S., & Prazeres, D. M. F. (2002). Isolation of plasmid DNA from cell lysates by aqueous two-phase systems. *Biotechnology and Bioengineering*, 78(4), 376–384. <https://doi.org/10.1002/BIT.10227>
 20. Luechau, F., Ling, T. C., & Lyddiatt, A. (2009a). Partition of plasmid DNA in polymer–salt aqueous two-phase systems. *Separation and Purification Technology*, 66(2), 397–404. <https://doi.org/10.1016/J.SEPPUR.2008.12.003>
 21. Wiendahl, M., Oelmeier, S. A., Dimer, F., & Hubbuch, J. (2012). High-throughput screening-based selection and scale-up of aqueous two-phase systems for p DNA purification. *Journal of Separation Science*, 35(22), 3197–3207. <https://doi.org/10.1002/jssc.201200310>
 22. Frerix, A., Müller, M., Kula, M.-R., & Hubbuch, J. (2005). Scalable recovery of plasmid DNA based on aqueous two-phase separation. *Biotechnology and Applied Biochemistry*, 42(1), 57–66. <https://doi.org/10.1042/ba20040107>
 23. Kepka, C., Rhodin, J., Lemmens, R., Tjerneld, F., & Gustavsson, P.-E. (2004). Extraction of plasmid DNA from *Escherichia coli* cell lysate in a thermoseparating aqueous two-phase system. *Journal of Chromatography A*, 1024, 95–104. <https://doi.org/10.1016/J.CHROMA.2003.10.028>
 24. Trindade, I. P., Diogo, M. M., Prazeres, D. M. F., & Marcos, J. C. (2005). Purification of plasmid DNA vectors by aqueous two-phase extraction and hydrophobic interaction chromatography. *Journal of Chromatography A*, 1082(2), 176–184. <https://doi.org/10.1016/J.CHROMA.2005.05.079>
 25. Gomes, G. A., Azevedo, A. M., Aires-Barros, R. M., & Prazeres, D. M. F. (2009). Purification of plasmid DNA with aqueous two phase systems of PEG 600 and sodium citrate/ammonium sulfate. *Separation and Purification Technology*, 65(1), 22–30. <https://doi.org/10.1016/J.SEPPUR.2008.01.026>
 26. Rahimpour, F., Feyzi, F., Maghsoudi, S., & Hatti-Kaul, R. (2006). Purification of plasmid DNA with polymer-salt aqueous two-phase system: optimization using response surface methodology. *Biotechnology and Bioengineering*, 95(4), 627–637. <https://doi.org/10.1002/bit.20920>
 27. Johansson, H.-O., Matos, T., Luz, J. S., Feitosa, E., Oliveira, C. C., Pessoa, A., Bülow, L., & Tjerneld, F. (2012). Plasmid DNA partitioning and separation using poly (ethylene glycol)/poly(acrylate)/salt aqueous two-phase systems. *Journal of Chromatography A*, 1233, 30–35. <https://doi.org/10.1016/J.CHROMA.2012.02.028>
 28. Matos, T., Johansson, H.-O., & Queiroz, J. A., Bulow, L. (2014). Isolation of PCR DNA fragments using aqueous two-phase systems. *Separation and Purification Technology*, 122, 144–148. <https://doi.org/10.1016/J.SEPPUR.2013.11.014>
 29. Janku, F., Huang, H. J., Pereira, D. Y., Kobayashi, M., Chiu, C. H., Call, S. G., Woodbury, K. T., Chao, F., Marshak, D. R., & Chiu, R. Y. T. (2021). A novel method for liquid-phase extraction of cell-free DNA for detection of circulating tumor DNA. *Scientific Reports*, 11(1), 19653. <https://doi.org/10.1038/s41598-021-98815-x>
 30. Nazer, B., Dehghani, M. R., & Goliaei, B. (2017). Plasmid DNA affinity partitioning using polyethylene glycol – sodium sulfate aqueous two-phase systems. *Journal of Chromatography B*, 1044–1045, 112–119. <https://doi.org/10.1016/J.JCHROMB.2017.01.002>
 31. Luechau, F., Ling, T. C., & Lyddiatt, A. (2011). Selective partition of plasmid DNA and RNA from crude *Escherichia coli* cell lysate by aqueous two-phase systems. *Biochemical Engineering Journal*, 55(3), 230–232. <https://doi.org/10.1016/j.bej.2011.04.014>
 32. Rito-Palomares, M., Dale, C., & Lyddiatt, A. (2000). Generic application of an aqueous two-phase process for protein recovery from animal blood. *Process Biochemistry*, 35(7), 665–673. [https://doi.org/10.1016/S0032-9592\(99\)00119-3](https://doi.org/10.1016/S0032-9592(99)00119-3)
 33. Oelmeier, S. A., Dimer, F., & Hubbuch, J. (2011). Application of an aqueous two-phase systems high-throughput screening method to evaluate mAb HCP separation. *Biotechnology and Bioengineering*, 108(1), 69–81. <https://doi.org/10.1002/bit.22900>
 34. Bensch, M., Selbach, B., & Hubbuch, J. (2007). High throughput screening techniques in downstream processing: Preparation, characterization and optimization of aqueous two-phase systems. *Chemical Engineering Science*, 62(7), 2011–2021. <https://doi.org/10.1016/j.ces.2006.12.053>
 35. Merchuk, J. C., Andrews, B. A., & Asenjo, J. A. (1998). Aqueous two-phase systems for protein separation. *Journal of Chromatography B*, 711, 285–293. [https://doi.org/10.1016/S0378-4347\(97\)00594-x](https://doi.org/10.1016/S0378-4347(97)00594-x)
 36. Glyk, A., Scheper, T., & Beutel, S. (2014). Influence of different phase-forming parameters on the phase diagram of several PEG-salt aqueous two-phase systems. *Journal of Chemical and Engineering Data*, 59(3), 850–859. <https://doi.org/10.1021/JE401002W>
 37. Zafarani-Moattar, M. T., & Jafari, P. (2013). Phase diagrams for liquid-liquid and liquid-solid equilibrium of the ternary polyethylene glycol+di-sodium hydrogen citrate+water system. *Fluid Phase Equilibria*, 337, 224–233. <https://doi.org/10.1016/j.fluid.2012.09.005>
 38. Eiteman, M. A. (1994). Partitioning of charged solutes in poly(ethylene glycol)/potassium phosphate aqueous two-phase systems. *Separation Science and Technology*, 29(6), 685–700. <https://doi.org/10.1080/01496399408005603>
 39. Walter, H., & Johansson, G. (1994). *Methods in enzymology: Aqueous two-phase systems* (Vol. 228). Academic Press, Inc.
 40. Asenjo, J. A., & Andrews, B. A. (2011). Aqueous two-phase systems for protein separation: A perspective. *Journal of Chromatography A*, 1218, 8826–8835. <https://doi.org/10.1016/j.chroma.2011.06.051>

41. Lis, J. T., & Schleif, R. (1975). Size fractionation of double-stranded DNA by precipitation with polyethylene glycol. *Nucleic Acids Research*, 2(3), 383–390.
42. Luechau, F., Ling, T. C., & Lyddiatt, A. (2009b). Selective partition of plasmid DNA and RNA in aqueous two-phase systems by the addition of neutral salt. *Separation and Purification Technology*, 68(1), 114–118. <https://doi.org/10.1016/J.SEPPUR.2009.04.016>
43. Johansson, H.-O., Karlström, G., Tjerneld, F., & Haynes, C. A. (1998). Driving forces for phase separation and partitioning in aqueous two-phase systems. *Journal of Chromatography B*, 711, 3–17. [https://doi.org/10.1016/S0378-4347\(97\)00585-9](https://doi.org/10.1016/S0378-4347(97)00585-9)
44. Albertsson, P.-A. (1986). *Partition of cell particles and macromolecules* (3rd ed.). John Wiley.
45. Frerix, A., Schönewald, M., Geilenkirchen, P., Müller, M., Kula, M.-R., & Hubbuch, J. (2006). Exploitation of the coil–globule plasmid DNA transition induced by small changes in temperature, pH salt, and poly(ethylene glycol) compositions for directed partitioning in aqueous two-phase systems. *Langmuir*, 22(9), 4282–4290. <https://doi.org/10.1021/la052745u>
46. Huddleston, J. (1991). The molecular basis of partitioning in aqueous two-phase systems. *Trends in Biotechnology*, 9(1), 381–388. [https://doi.org/10.1016/0167-7799\(91\)90130-A](https://doi.org/10.1016/0167-7799(91)90130-A)
47. Marcos, J. C., Fonseca, L. P., Ramalho, M. T., & Cabral, J. M. S. (1999). Partial purification of penicillin acylase from *Escherichia coli* in poly(ethylene glycol)–sodium citrate aqueous two-phase systems. *Journal of Chromatography B*, 734, 15–22. [https://doi.org/10.1016/S0378-4347\(99\)00319-9](https://doi.org/10.1016/S0378-4347(99)00319-9)
48. Buzanovskii, V. A. (2017). Determination of proteins in blood. Part 1: Determination of total protein and albumin. *Review Journal of Chemistry*, 7(1), 79–124. <https://doi.org/10.1134/S2079978017010010>
49. Nazer, B., Dehghani, M., Goliaei, B., & Morad, E. (2017). Partitioning of pyrimidine single stranded oligonucleotide using polyethylene glycol – sodium sulfate aqueous two-phase systems; experimental and modeling. *Fluid Phase Equilibria*, 432, 45–53. <https://doi.org/10.1016/J.FLUID.2016.10.014>

SUPPORTING INFORMATION

Additional supporting information can be found online in the Supporting Information section at the end of this article.

How to cite this article: Meutelet, R., Bisch, L. J., Buerfent, B. C., Müller, M., & Hubbuch, J. (2024). Partitioning behavior of short DNA fragments in polymer/salt aqueous two-phase systems. *Biotechnology Journal*, 19, e2400394. <https://doi.org/10.1002/biot.202400394>